

(salen)Mn^{III} Compounds as Nonpeptidyl Mimics of Catalase. Mechanism-Based Tuning of Catalase Activity: A Theoretical Study

Yuri G. Abashkin* and Stanley K. Burt

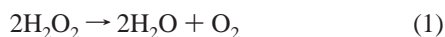
Advanced Biomedical Computing Center, SAIC-Frederick, Inc., National Cancer Institute at Frederick, P.O. Box B, Frederick, Maryland 21702-1201

Received September 14, 2004

We present the results of the first theoretical investigation of salen–manganese complexes as synthetic catalytic scavengers of hydrogen peroxide molecules that mimic catalase enzymes. Catalase mimics can be used as therapeutic agents against oxidative stress in treatment of many diseases, including Alzheimer's disease, stroke, heart disease, aging, and cancer. A ping-pong mechanism approach has been considered to describe the H₂O₂ dismutation reaction. The real compounds reacting with a peroxide molecule were utilized in our BP density functional calculations to avoid uncertainties connected with using incomplete models. Part I of the dismutation reaction—converting a peroxide molecule into a water molecule with simultaneous oxidation of the metal atom of the catalyst—can be done quite effectively at the Mn catalytic center. To act as catalytic scavengers of hydrogen peroxide, the oxomanganese salen complexes have to be deoxidized during part II of the dismutation reaction. It has been shown that there are two possible reaction routes for the second part of the dismutation reaction: the top and the side substrate approach routes. Our results suggest that the catalyst could be at least temporarily deactivated (poisoned) in the side approach reaction route due to the formation of a kinetically stable intermediate. Overall, the side approach reaction route for the catalyst recovery is the bottleneck for the whole dismutation process. On the basis of the detailed knowledge of the mode of action of the (salen)Mn^{III} catalase mimics, we suggest and rationalize structural changes of the catalyst that should lead to better therapeutic properties. The available experimental data support our conclusions. Our findings on the reaction dismutation mechanism could be the starting point for further improvement of salen–manganese complexes as synthetic catalytic scavengers of reactive oxygen species.

Introduction

Reactive oxygen species are inevitably formed during the metabolism of oxygen in aerobic organisms. Many disease states can be broadly characterized as ones in which the body fails to adequately resist the overproduction of undesired reactive oxygen species. Hydrogen peroxide is one such undesired metabolic byproduct in living systems. For the degradation of this reactive oxygen species, organisms use catalase enzymes^{1,2} which effectively dismutate H₂O₂ according to the following:³



Hydrogen peroxide can be produced at increased levels in a

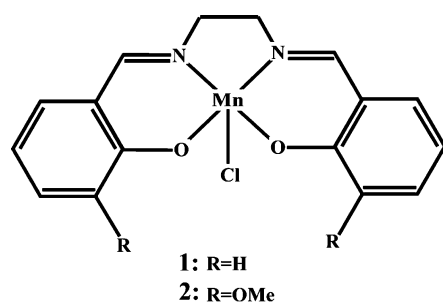
variety of pathological situations. If the production of H₂O₂ overwhelms the activity of catalase enzymes, then H₂O₂ becomes the substrate for the Fenton reaction, resulting in extremely toxic and mutagenic hydroxyl radicals (OH[•]).⁴ To avoid this situation, synthetic antioxidants, which scavenge excess oxidants, can be used as therapeutic agents against oxidative stress. An incomplete list of possible applications of antioxidants include treatment of Alzheimer's disease,⁵ stroke,⁶ heart disease,⁷ aging,^{8,9} and cancer.¹⁰

* Author to whom correspondence should be addressed. E-mail: abashkin@ncifcrf.gov.

- (1) Schonbaum, G. R.; Chance, B. In *The Enzymes*; Academic Press: New York, 1976; Vol. 13, p 363.
- (2) Kalko, S. G.; Gelpi, J. L.; Fita, I.; Orozco, M. *J. Am. Chem. Soc.* **2001**, *123*, 9665–9672.
- (3) Zamocky, M.; Koller, F. *Prog. Biophys. Mol. Biol.* **1999**, *72*, 19–66 and references therein.

- (4) Helliwell, B.; Gutteridge, J. M. C. *Free Radicals in Biology and Medicine*, 2nd ed.; Clarendon Press: Oxford, U.K., 1993; pp 1–21.
- (5) Smith, M. A.; Rottkamp, C. A.; Nunomura, A.; Raina, A. K.; Perry, G. *Biochim. Biophys. Acta* **2000**, *1502*, 139–144.
- (6) Baker, K.; Marcus, C. B.; Huffman, K.; Kruk, H.; Malfroy, B.; Doctrow, S. R. *J. Pharmacol. Exp. Ther.* **1998**, *284*, 215–221.
- (7) Reilly, M. P.; Delanty, N.; Roy, L.; Rokach, J.; Callaghan, P. O.; Crean, P.; Lawson, J. A.; FitzGerald, G. A. *Circulation* **1997**, *96*, 3314–3320.
- (8) Melov, S.; Ravenscroft, J.; Malik, S.; Gill, M. S.; Walker, D. W.; Clayton, P. E.; Wallace, D. C.; Malfroy, B.; Doctrow, S. R.; Lithgow, G. *Science* **2000**, *289*, 1567–1569.
- (9) Taub, J.; Lau, J. F.; Ma, C.; Hahn, J. H.; Hoque, R.; Rothblatt, J.; Chalfie, M. *Nature* **1999**, *399*, 162–166.

Chart 1



A number of research groups have been developing low molecular weight catalysts (biomimetics) that mimic natural enzyme functions to suppress various reactive oxygen species, including peroxide.^{11,12} Catalase mimics were built around iron(III),^{13–15} dinuclear manganese,^{16–20} and Mn(III) centers.^{21–23} The latter—(salen)Mn^{III} compounds (Chart 1)—have been proven to be especially promising as therapeutics.^{8,21} These complexes are also known as synthetic asymmetric catalysts that are important alternative to enzymes because they provide high enantioselectivity control and in contrast to biological catalysts can be used with a wide range of substrates.^{24–26} The distinctive feature of the salen–manganese complexes that makes their broad pharmacological efficacy possible is the ability to mimic both catalase and superoxide dismutase enzymatic functions.^{22,27} Remarkably, different salen–manganese compounds possess the same superoxide dismutase activity but may significantly differ in the catalase activity. For example, it was shown²⁸ that compound **2** is much more effective as a catalase than compound **1**.

Though significant therapeutic and chemical information on the salen–manganese catalase mimics has been accumulated from extensive experimental studies,^{21–23} a detailed picture of the peroxide dismutation at the molecular level is yet to be obtained. An understanding of the mechanism of the dismutation process is an important basis for rational design and tuning these analogues to yield better therapeutic properties. From a fundamental point of view, the study of the catalytic mechanism of the functional biomimetics of enzymes might contribute to a better understanding of the complex enzymatic activities for the corresponding biological compounds. In this paper, we present the first theoretical investigation of salen–manganese complexes as catalytic scavengers of hydrogen peroxide molecules. It is also shown that understanding the reaction leads to mechanism-based tuning suggestions of how to increase catalase activities of the salen–manganese complexes.

It was suggested by us³⁰ that Mn^V=O can be the active intermediate species in the dismutation process. Generation of the Mn–oxo intermediates via heterolytic cleavage of H₂O₂ has been reported in (salen)Mn-catalyzed alkene epoxidation with peroxide,³¹ supporting our computational conclusion on the feasibility of such manganese atom oxidation by a peroxide molecule. All mentioned above, however, does not rule out that other reactive species (like Mn(IV)) that are formed via homolytic cleavage of the O–O peroxide bond can be involved in the dismutation, though their presence in the case of the epoxidation reaction simply results in deactivation of (salen)Mn catalyst and should be avoided.³² One can find examples of radical reaction routes in the case of binuclear manganese and heme catalases in recent publications.^{12,33,34} In this work we concentrate our efforts on the dismutation reactions with Mn–oxo intermediates.

We consider (Figure 1) a general “ping-pong” mechanism approach²⁹ to describe the reaction process in which the first molecule of H₂O₂ binds to the metal center (Mn(III)), oxidizes the metal, and releases a molecule of water (I). The second peroxide molecule approaches the oxomanganese intermediate compound (Mn(V)), and the oxygen atom is transferred back to the peroxide molecule forming O₂ and H₂O (II). The first part of the reaction was recently studied by us.³⁰ Our findings suggest (Figure 1) that the first part of the dismutation reaction—the metal oxidation by a peroxide molecule—is a one-step process. The concerted breaking of the O–O peroxide bond, oxidation of the Mn, and water molecule formation occur on the triplet state potential energy

- (10) Kong, Q.; Beel, J. A.; Lillehei, K. O. *Med. Hypotheses* **2000**, *55*, 29–35.
- (11) Riley, D. P. *Chem. Rev.* **1999**, *99*, 2573–2587.
- (12) Wu, A. J.; Penner-Hahn, J. E.; Pecoraro, V. L. *Chem. Rev.* **2004**, *104*, 903–938 and references therein.
- (13) Paschke, J.; Kirsch, M.; Korth, H.-G.; de Groot, H.; Sustmann, R. *J. Am. Chem. Soc.* **2001**, *123*, 11099–11100.
- (14) Robert, A.; Look, B.; Momenteau, M.; Meunier, B. *Inorg. Chem.* **1991**, *30*, 706–711.
- (15) Murata, K.; Panicucci, R.; Yopinath, P.; Bruce, T. C. *J. Am. Chem. Soc.* **1990**, *112*, 6072–6083.
- (16) Gerasimchuk, N. N.; Gerges, A.; Clifford, T.; Danby, A.; Bowman-James, K. *Inorg. Chem.* **1999**, *38*, 5633–5636.
- (17) Triller, M. U.; Hsieh, W.-Y.; Pecoraro, V. L.; Rompel, A.; Krebs, B. *Inorg. Chem.* **2002**, *41*, 5544–5554.
- (18) Romero, I.; Dubois, L.; Collomb, M.-N.; Deronzier, A.; Latour, J.-M.; Pecaat, J. *Inorg. Chem.* **2002**, *41*, 1795–1806.
- (19) Boelrijk, A. E. M.; Khangulov, S. V.; Dismukes, G. C. *Inorg. Chem.* **2000**, *39*, 3009–3019.
- (20) Brunold, T. C.; Gamelin, D. R.; Solomon, E. I. *J. Am. Chem. Soc.* **2000**, *122*, 8511–8523.
- (21) Doctrow, S. R.; Huffman, K.; Marcus, C. B.; Musleh, W.; Bruce, A.; Baudry, M.; Malfroy, B. In *Antioxidants in Disease: Mechanisms and Therapy*; Sies, H., Ed.; Academic Press: San Diego, CA, 1997; pp 247–269.
- (22) Rong, Y.; Doctrow, S. R.; Tocco, G.; Baudry, M. *Proc. Natl. Acad. Sci. U.S.A.* **1999**, *96*, 9897–9902.
- (23) Giblin, G. M.; Box, P. C.; Campbell, I. B.; Hancock, A. P.; Roomans, S.; Mills, G. I.; Molloy, C.; Tranter, G. E.; Walker, A. L.; Doctrow, S. R.; Huffman, K.; Malfroy, B. *Bioorg. Med. Chem. Lett.* **2001**, *11*, 1367–1370.
- (24) Jacobsen, E. N. In *Catalytic Asymmetric Synthesis*, 1st ed.; Ojima, I., Ed.; VCH: New York, 1993; pp 159–202.
- (25) Katsuki, T. *Coord. Chem. Rev.* **1995**, *140*, 189–214.
- (26) Dalton, C. T.; Rayn, K. M.; Wall, V. M.; Bousquet, C.; Gilheany, D. G. *Top. Catal.* **1998**, *5*, 75–9.
- (27) Superoxide dismutase converts a superoxide anion to harmless byproducts (for details see, for example, ref 11).

- (28) Doctrow, S. R.; Huffman, K.; Marcus, C. B.; Tocco, G.; Malfroy, E.; Adinolfi, C. A.; Kruk, H.; Baker, K.; Lazarowycz, N.; Mascarenhas, J.; Malfroy, B. *J. Med. Chem.* **2002**, *45*, 4549–4558.
- (29) Maté, M. J.; Murshudov, G.; Bravo, J.; Melik-Adamyany, W.; Loewen, P. C.; Fita, I. In *Handbook of Metalloproteins*; Messerschmidt, A., Huber, R., Eds.; John Wiley: New York, 2001.
- (30) Abashkin, Y. G.; Burt, S. K. *J. Phys. Chem. B* **2004**, *108*, 2708–2711.
- (31) Berkessel, A.; Frauenkron, M.; Schwenkreis, T.; Steinmetz, A.; Baum, G.; Fenske, D. *J. Mol. Catal., A: Chem.* **1996**, *113*, 321–342.
- (32) Lane, B. S.; Burgess, K. *Chem. Rev.* **2003**, *103*, 2457–2473.
- (33) Siegbahn, P. E. M. *Theor. Chem. Acc.* **2001**, *105*, 197–206.
- (34) Holm, R. H.; Kennepohl, P.; Solomon, E. I. *Chem. Rev.* **1996**, *96*, 2239–2314.

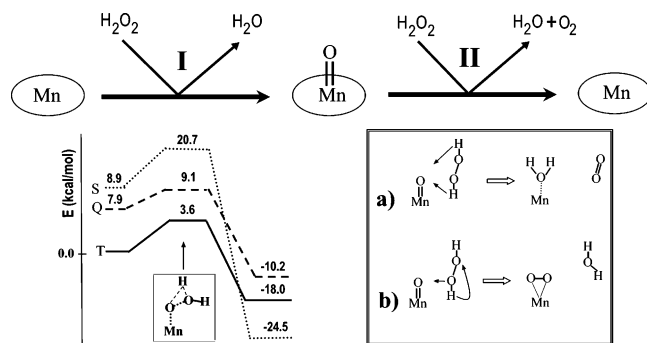


Figure 1. Ping-pong mechanism for dismutation of an H₂O₂ molecule by (salen)Mn^{III} catalase mimic: (I) the metal oxidation by a peroxide molecule; (II) conversion of the second peroxide molecule into O₂ and H₂O with simultaneous deoxygenation of the Mn atom (recovering the salen catalyst). The energetic reaction profiles that correspond to the concerted breaking of the O–O peroxide bond, oxidation of the Mn, and water molecule formation are shown below step I as they were calculated in our previous work.³⁰ Two possible mechanistic schemes for step II are shown: (a) intermolecular transfers of the hydrogen peroxide protons to the oxidizing oxomanganese salen atom; (b) intramolecular hydrogen peroxide proton transfer with simultaneous formation of an oxygen–oxygen bond between the atoms of the salen and the peroxide moieties.

surface. This process involves an intramolecular proton transfer that can be done effectively at the Mn catalytic center (the reaction TS barrier = 3.6 kcal/mol). In this paper we study step II of the dismutation reaction and, on the basis of our findings, analyze the whole reaction 1. Two possible mechanistic schemes (Figure 1) for converting H₂O₂ into H₂O and O₂ with simultaneous deoxygenation of the Mn atom are considered: intermolecular transfer of the hydrogen peroxide protons to the oxygen atom of the oxomanganese compound (a) and the intramolecular hydrogen peroxide proton transfer with simultaneous formation of the oxygen–oxygen bond between the corresponding atoms of the salen–manganese and peroxide moieties (b). Both mechanisms lead to the same products (though differently situated in the final complexes): a molecule of water and a molecule of oxygen. Importantly, the real compounds **1** and **2** reacting with a peroxide molecule were utilized in our density functional calculations to avoid uncertainties connected with using incomplete models.

Method

All DFT calculations of the different reaction pathways were carried out using the DGauss program³⁵ as implemented in UniChem 4.0.³⁶ The calculations were performed using DZVP basis sets, which are (621/41/1) for carbon, oxygen, and nitrogen atoms, (41) for hydrogen atoms, and (6321/411/1) for the manganese atom.^{37,38} The nonlocal corrections using the Becke exchange³⁹ and Perdew correlation⁴⁰ potentials have been obtained starting from the Vosko, Wilk, and Nuisar local potential⁴¹ (BP86 DFT functional).

- (35) Andzelm, J.; Wimmer, E. *J. Chem. Phys.* **1992**, *96*, 1280–1303.
 (36) UniChem V4.0; Oxford Molecular: Medawar Center, Oxford Science Park, Oxford, OX4 4GA, England.
 (37) Sosa, C.; Andzelm, J.; Elkin, B. C.; Wimmer, E.; Dobbs, K. D.; Dixon, D. A. *J. Phys. Chem.* **1992**, *96*, 6630–6636.
 (38) Godbout, N.; Salahub, D. R.; Andzelm, J.; Wimmer, E. *Can. J. Chem.* **1992**, *70*, 560–571.
 (39) Becke, A. D. *Phys. Rev.* **1988**, *A38*, 3098–3100.
 (40) Perdew, J. P. *Phys. Rev.* **1986**, *B33*, 8822–8824.

Nonhybrid BP86 and hybrid B3LYP DFT functionals have been used by different groups of researchers to make valuable insights into various aspects of the (salen)Mn catalytic systems.^{30,42–46} The advantages and disadvantages of using BP86 and B3LYP approximations for these catalytic systems are hotly debated. There is a growing understanding that both DFT approaches are not the ideal tools for precise quantitative characterization of these systems.^{46–48} In particular, B3LYP can significantly overestimate the stability of the quintet state, while BP86 may need correction of the TS barrier values. From our point of view, these quantitative uncertainties should not prevent use of the DFT method (that is presently the only practical approach for such systems) for investigation of Mn–salen reactivity, providing that researchers concentrate their attention on qualitative conclusions/chemical concepts derived from relative comparison of the reaction species and mechanisms. In addition, of course, warnings should be given in case any doubts exist that quantitative accuracy of the approach used might influence qualitative conclusions. Obtained in such a way, results could be helpful for experimentalists and might be the starting points for future, more precise calculations that would use high level ab initio methods or improved DFT functionals. We use in this work BP86 density functional that leads to conclusions that do not contradict the qualitative picture of spin state pattern derived from high-level ab initio calculations⁴⁷ of oxo–manganese species. The use of pure density functionals for (salen)Mn catalysts was also recommended in the recent paper⁴⁸ based on comparison between various DFT functionals.

For every stationary point, an analytical Hessian matrix⁴⁹ was calculated to prove the nature of the optimized structure. All calculations were performed using the unrestricted Hartree–Fock formalism. We discuss the reaction in terms of internal energy profiles.

Results and Discussion

The reaction of converting H₂O₂ into H₂O and O₂ with simultaneous deoxygenation of the Mn atom of the oxomanganese salen **1** complex has been calculated on the three different spin potential energy surfaces: the singlet, the triplet, and the quintet. The singlet state has been found to be the ground state for the initial reaction complexes followed by the triplet and the quintet states. Two reaction initial conformations have been discovered in the process of searching local minima on the reaction potential energy surface.

Initial Complexes for the Reaction between the Oxomanganese–salen Compound and a Peroxide Molecule. Optimized structures for two possible conformations of the initial reaction complexes are shown in Figure 2. The first structure corresponds to the top approach of a peroxide

- (41) Vosko, S. H.; Wilk, L.; Nusair, M. *Can. J. Phys.* **1980**, *58*, 1200–1211.
 (42) Cavallo, L.; Jacobsen, H. *Inorg. Chem.* **2004**, *43*, 2175–2182.
 (43) Cavallo, L.; Jacobsen, H. *J. Org. Chem.* **2003**, *68*, 6202–6207.
 (44) Abashkin, Y. G.; Burt, S. K. *Org. Lett.* **2004**, *6*, 59–62.
 (45) Khavrutskii, I. V.; Musaev, D. G.; Morokuma, K. *J. Am. Chem. Soc.* **2003**, *125*, 13879–13889.
 (46) Khavrutskii, I. V.; Rahim, R. R.; Musaev, D. G.; Morokuma, K. *J. Phys. Chem. B* **2004**, *108*, 3845–3854.
 (47) Abashkin, Y. G.; Collins, J. R.; Burt, S. K. *Inorg. Chem.* **2001**, *40*, 4040–4048.
 (48) Jacobsen, H.; Cavallo, L. *Phys. Chem. Chem. Phys.* **2004**, *6*, 3747–3753.
 (49) Komornicki, A.; Fitzgerald, G. *J. Chem. Phys.* **1993**, *98*, 1398–1421.

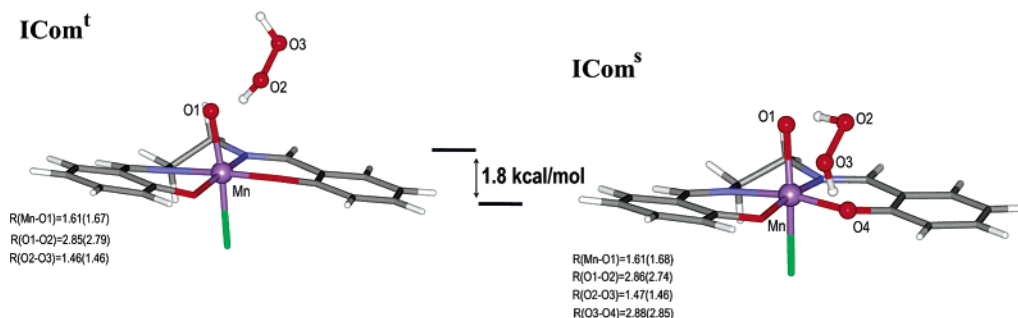


Figure 2. Initial complexes for the reaction between the oxomanganese salen compound and a peroxide molecule: (ICom^t) initial complex corresponding to the top approach of the substrate; (ICom^s) initial complex corresponding to the side approach of the substrate. The energetic difference between two initial complexes (1.8 kcal/mol) is also shown. Selected optimized geometrical parameters are shown for the singlet state. The corresponding parameters for the triplet state are shown in parentheses. Bond lengths are in angstroms.

molecule to the plane of the catalase mimic. Such an approach leads to the formation of only one hydrogen bond between the O2 atom of the peroxide and the O1 axial oxygen atom of the oxomanganese compound (Figure 2, ICom^t). In this initial complex the substrate is situated in a “pop-up” position with respect to the catalyst plane. In contrast, the side approach of a peroxide molecule to the salen compound results in a stable complex ICom^s (Figure 2) that not only has a hydrogen bond between the O1 oxidizing atom of the catalyst and the O2 atom of the peroxide but also has the second hydrogen bond between the O3 atom of the peroxide and the O4 atom of the salen moiety. It is interesting to note that the energetic difference between these two initial complexes in the ground singlet state is just 1.8 kcal/mol with the complex ICom^s being more stable than the complex ICom^t . Such a small energetic difference may be surprising at the first glance because complex ICom^s has one more hydrogen bond in comparison with complex ICom^t . One, however, has to take into account the destabilizing electrostatic interaction between the O3 atom of the peroxide and the axial and equatorial oxygen atoms of the salen compound. These interactions are absent in the pop-up initial complex structure ICom^t . Overall, we conclude that the top and the side complexes are both accessible as starting conformations for this reaction. We will show that the mechanistic picture of the reaction strongly depends on what initial complex the reaction originates from.

Top Approach Reaction Pathways. The energetic profiles for the reaction starting from the pop-up initial complexes (Figure 3) have been calculated for two different mechanisms: a and b (Figure 1).

Geometrical parameters of the concerted transition state (TS) and the final complex structures for the intramolecular proton-transfer mechanism b can be found in Figure 4.

The optimized geometries of the reaction critical points that are related to the intermolecular proton-transfer mechanism a on the singlet, triplet, and quintet potential energy surfaces are shown in Figure 5.

As can be seen from Figure 3, the concerted intramolecular proton transfer in the peroxide compound and the simultaneous creation of an oxygen molecule from the O1 and O2 atoms of the salen and the peroxide moieties (Figure 4, TScon^t) need more than 50 kcal/mol of activation energy.

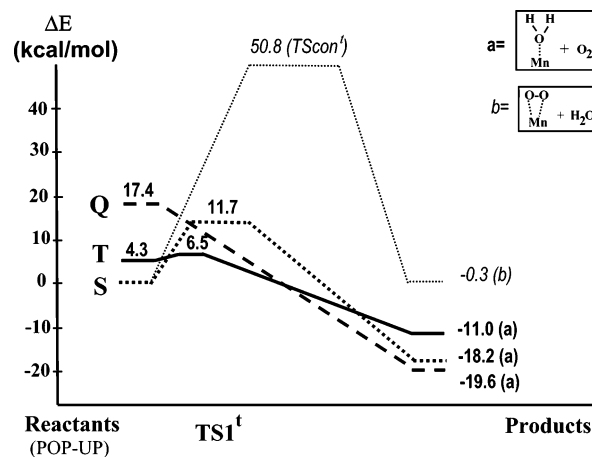


Figure 3. Reaction profiles in the case of the top approached substrate. Relative reaction energies of the triplet, the quintet, and the singlet reaction pathways are shown for mechanism a.⁵⁰ The singlet state reaction profile is shown for the concerted mechanism b.

Such a high TS barrier makes mechanism b energetically forbidden for the dismutation reaction.

In contrast, the transfer of the protons from a peroxide molecule to the oxidizing oxygen atom of the oxomanganese salen compound (mechanism a) can be done relatively easily. In the singlet state, which is the resting state of the reactants, a modest 11.7 kcal/mol activation energy is needed to overcome the TS barrier for the transfer of the first proton from the substrate (Figures 3 and 5, TS1^t). The triplet and quintet reaction channels are even more reactive: only a 2.2 kcal/mol barrier exists on the triplet path; there is no barrier in the quintet state. Potentially, mechanism a is a stepwise process with the transfers of the first and the second protons and could be separated by the presence of a reaction intermediate. However in the case of this reaction, no intermediate structures have been found for the three spin channels. The reaction coordinate shows that after overcoming TS1^t barrier in the singlet and in the triplet states the intermediate reaction moiety H–O3–O2 (Figure 5) simply approaches the O1 axial atom of the Mn–salen compound and surrenders the second proton to the O1 atom without any barrier. In the quintet state not only is the second proton-transfer barrierless but, as we mentioned, the initial protonation of the axial salen oxygen is also spontaneous.

In this reaction, a water molecule H–O1–H coordinated to the Mn atom and a molecule of oxygen O2–O3 are

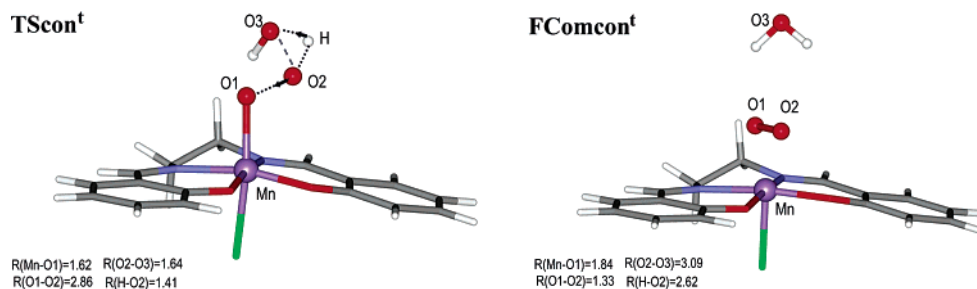


Figure 4. Optimized critical reaction structures for the concerted mechanism b in the case of the top approach of the substrate (in the singlet state): (TScon[†]) transition state leading to the final product complex FComcon[†]. Bond lengths are in angstroms.

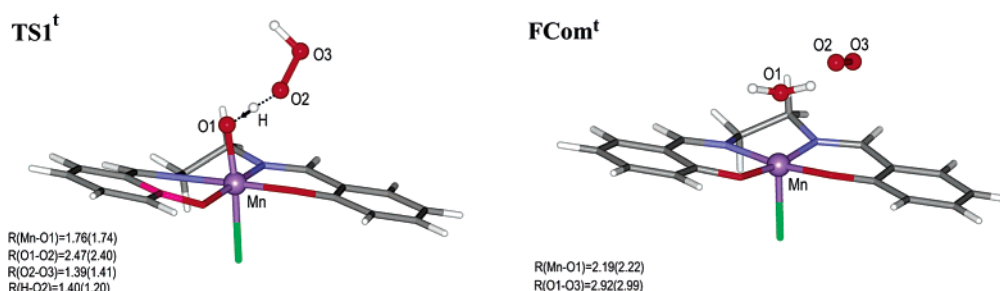


Figure 5. Optimized critical reaction structures for the stepwise mechanism a in the case of the top approach of the substrate: (TS1[†]) transition state leading to the final product complex FCom[†]. No stable intermediate has been found on the reaction pathways after the first proton transfer from the peroxide toward the oxomanganese salen compound (see the text for details). Selected geometrical parameters are shown for the singlet state. The corresponding parameters for the triplet state are shown in parentheses. Bond lengths are in angstroms.

formed as the reaction products (Figure 5, FCom[†]). Overall, mechanism a in the case of the top approach of the substrate is a one-step process.

It is interesting to observe spin population changes on the metal site and the O–O moiety of a peroxide molecule in the process of the reaction product ((salen)Mn^{III} and the triplet O₂ compounds⁵⁰) formation. The reaction starts with zero, two, and four unpaired electrons located on the catalyst for the singlet, the triplet, and the quintet channels, respectively, and with no spin density on the peroxide molecule. For the singlet and the triplet processes that overcome activation barriers the spin population analysis shows formation of spin densities on the O–O peroxide moiety (0.56 and 0.35; spin up) in the vicinity of the transition state structures. The corresponding opposite spin densities (spin down) are formed on the catalyst site.

Side Approach Reaction Pathways. The side approach reaction pathways have been investigated in the same manner as we did for the top approach of a peroxide molecule. The energetic reaction profiles and the optimized structures of the reaction critical points for mechanisms b and a are shown in Figures 6–8, respectively.

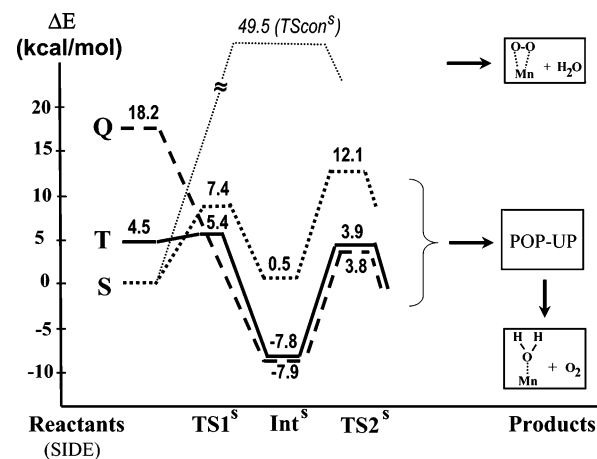


Figure 6. Reaction profiles in the case of the side approached substrate. Relative reaction energies of the triplet, the quintet, and the singlet reaction pathways are shown for mechanism a. The singlet state reaction profile is shown for the concerted mechanism b.

Because of the very high barrier (49.5 kcal/mol) for the activation of the concerted process (Figures 6 and 7), we consider mechanism b to be unfeasible for the dismutation reaction.

The reaction that follows mechanism a can be described as a number of steps starting from the initial reactant conformation Icom^s (Figure 2). First, the proton is transferred from the substrate to the O1 atom of the salen compound (Figure 8, TS1^s) resulting in the reaction intermediate Int^s. For this intermediate structure the quintet and the triplet states are almost degenerated. They lie ~8 kcal/mol lower than the singlet state, which is the resting state for the reactants. This indicates that spin-crossing occurs for the different spin reaction pathways between TS1^s and Int^s. To finish the reaction, that is to transfer the second proton to the O1 atom

(50) For all mechanism a channels the formation of the triplet O₂ molecule is observed in the final complexes: O₂ spin densities for the singlet, the triplet, and the quintet channels are 1.86, 1.82, and 2.01. Correspondingly, Mn spin densities are 1.83, 0.14, and 1.81. The possibility of four unpaired electrons on the metal site has been also investigated. Such a septet complex lies 10.7 kcal/mol higher than the quintet one. However, for the separated product moieties the quintet and the triplet represent degenerated ground states for (salen)Mn catalyst. The relative under-stabilization of the (salen)Mn final complexes containing the quintet spin state on the metal has been also observed in the case of the catalyzed epoxidation reaction of alkenes. The diminished coordination of the epoxide to the metal⁴⁷ (the pair of a water and an oxygen molecules in this case) is the reason for such a result.

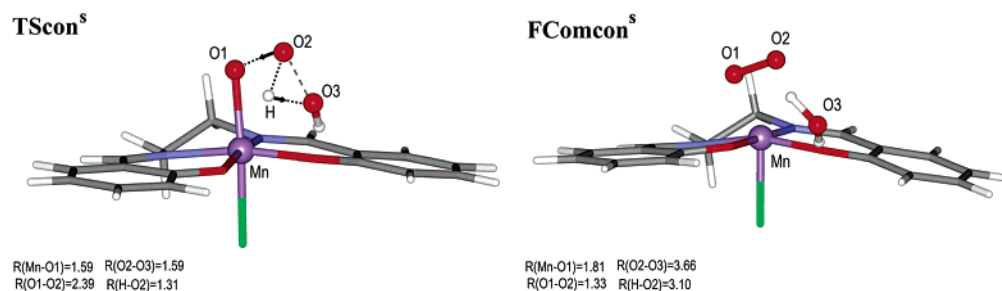


Figure 7. Optimized critical reaction structures for the concerted mechanism b in the case of the side approach of the substrate (in the singlet state): (TScon^s) transition state leading to the final product complex FComcon^s. Bond lengths are in angstroms.

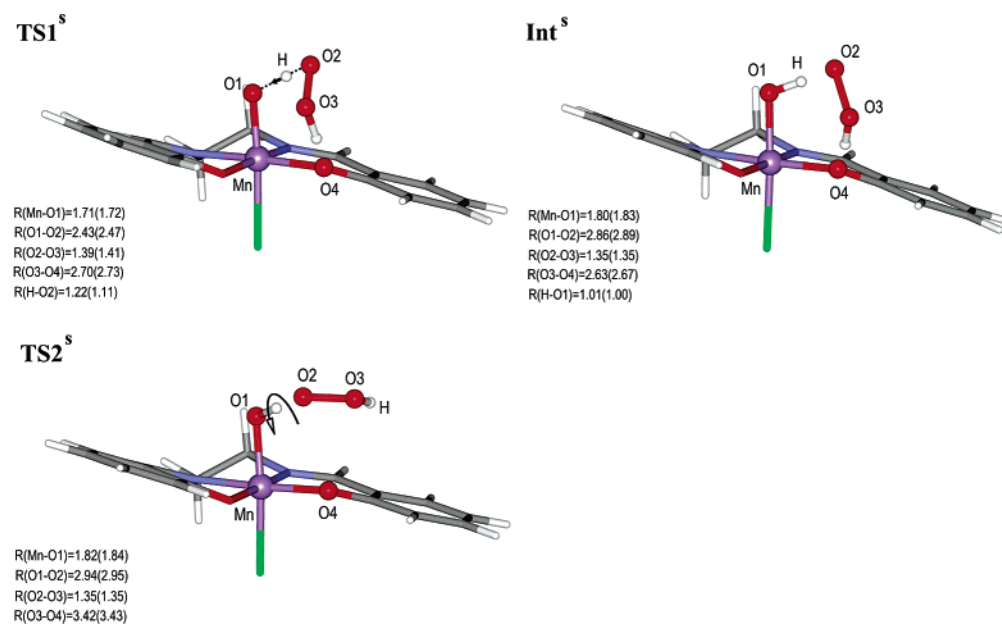


Figure 8. Optimized critical reaction structures for the stepwise mechanism a in the case of the side approach of the substrate: (TS1^s) transition state leading to the reaction intermediate Int^s; (TS2^s) transition state resulting in “pop-up” conformation of the O2–O3–H substrate moiety. After the last step the reaction follows the top approach pathways (see above). Selected geometrical parameters are shown for the singlet state. The corresponding parameters for the triplet state are shown in parentheses. Bond lengths are in angstroms.

of the catalyst, the hydrogen bond O3–H–O4 between the salen framework and the peroxide moiety has to be broken and the O2–O3–H peroxide part must be moved into the pop-up position with respect to the catalyst plane. This can be done through transition state TS2^s. Roughly speaking, the transition structure can be reached with rotating the peroxide moiety about the O1–O2 axis (Figure 8). Approximately the same barrier of 12 kcal/mol for every spin state has to be overcome to perform this reaction step. As soon as the O2–O3–H peroxide moiety is in the pop-up position, transfer of the second proton is a barrierless process in all three spin states as we discussed for the top approach reaction pathways.

It should be mentioned that for every reaction channel spin populations are virtually the same (with accuracy of several hundreds of an electron unit) for the TS1^s, INT^s, and TS2^s structures. Moreover, spin densities on the O–O part of the peroxide moiety for different channels are very similar as well. For the intermediates they are 1.01, 1.2, and 1.2 (all are spin up) for the singlet, the triplet, and the quintet. Corresponding Mn spin densities are 1.03 (spin down), 2.6 (spin down), and 2.6 (spin up).

Comparison of the Top and Side Substrate Approach Reaction Routes. Mechanism-Based Tuning of Catalase Activity of salen–Manganese Complexes. The results of our calculations show that only mechanism a, which requires two intermolecular transfers of the hydrogen peroxide protons to the oxidizing oxomanganese salen atom, is feasible for the both reaction routes: the top and the side approach of a peroxide molecule to the plane of the catalase mimic. The mechanistic pictures for these two reactions are quite different. The top approach reaction is a one-step process while the product formation in the case of the side approach of a peroxide molecule needs several steps. The only similarity between these reaction routes is the same qualitative and quantitative picture for the first proton-transfer step. This reaction step can be considered as a spin-forbidden one and can be done very effectively by assuming a spin change during the reaction progress. It is interesting to note that theoretical and experimental studies have recently led to the finding that (salen)Mn-catalyzed epoxidation of alkenes is also a multichannel process with different spin states and the possible crossing of potential energy surfaces.^{44,47,51–54} There are two possible scenarios involving the spin change

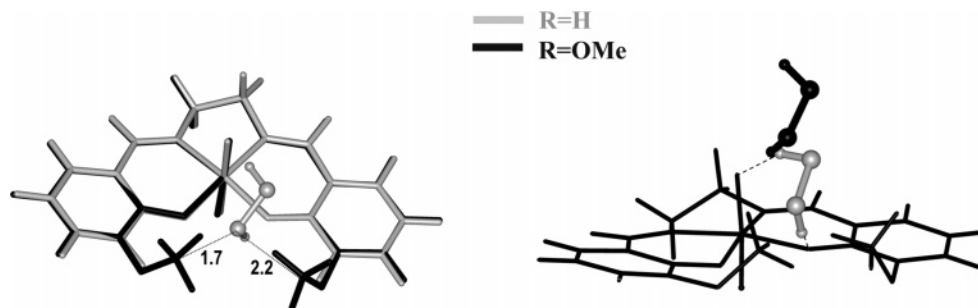


Figure 9. Superposition of the optimized structure of the compound **1** with a peroxide molecule and compound **2** (left picture) and results of the optimization of the peroxide molecule position for compound **2** (right picture). The initial position of a peroxide molecule corresponds to compound **1** and is shown in gray.

in the course of the dismutation reaction. The first way is the excitation of the initial complex from the singlet to the triplet state (needs 4.3 and 4.5 kcal/mol for the top and the side route, respectively) followed by overcoming the triplet **TS1** barrier (2.2 and 0.9 kcal/mol). The total activation energy needed is therefore only 6.5 kcal/mol for the top approach reaction and only 5.4 kcal/mol for the side approach reaction.⁵⁵ Spin-crossing effects (multispin reactivity^{56–58}) can also lead to decreasing the effective reaction barrier since the initial singlet state likely changes to the lower triplet (or quintet) state en route to the singlet **TS1**. Very similar geometries of the reaction critical points in the different spin states (Figures 2, 5, and 8) should facilitate the spin changing.

The principal difference of the side approach reaction route from the top one is the presence of a kinetically stable intermediate structure **Int^s** that appears on the reaction path after the first protonation of the O1 atom. The depth of the local minimum corresponding to this intermediate is ~12 kcal/mol for the lowest triplet and the quintet states. This depth estimation should be regarded as a minimal one since DFT has some tendency to underestimate TS barriers. Thus, intermediate **Int^s** can be considered as an “energetic trap” on the reaction path, making the side approach route much less efficient than the one-step top approach transformation of a peroxide molecule.

As we showed in our previous work,³⁰ part I of the dismutation reaction (Figure 1)—converting a peroxide molecule into a water molecule with simultaneous oxidation of the metal atom of the catalyst—can be done quite effectively at the Mn catalytic center (the reaction TS barrier = 3.6 kcal/mol). To act as a catalytic scavenger of hydrogen peroxide agents, the oxomanganese salen complex has to be

deoxidized in the course of part II of the dismutation reaction. Our results suggest that the side approach reaction route for the catalyst recovery is the bottleneck for the whole dismutation reaction that follows a ping-pong mechanism. In other words, the catalyst could be at least temporarily deactivated (poisoned) if it entered the side approach reaction route due to formation of kinetically stable byproduct **Int^s**.

It is intriguing to speculate that blocking the side approach reaction route should lead to increasing the catalase activity of the (salen)Mn^{III} compound. We suggest that bulky substituents at 3 and 3' positions of the salen ligand could block access of a peroxide molecule to the equatorial oxygen atoms of the salen framework. The latter should preclude formation of the side approach initial reaction complex and “turn off” the side approach route. Indeed, the experimental evidence²⁸ suggests that substitution of the hydrogen atoms at 3 and 3' positions with R=O–CH₃ groups (Chart 1, compound **2**) dramatically improves the catalase activity of the salen biomimetic. Our additional modeling illustrates how this substitution might shut down the side approach reaction route.

First, as can be seen from Figure 9, a peroxide molecule collides with the carbon atoms of OMe groups in compound **2** if the peroxide molecule is situated in the position optimized for the side initial complex in the compound **1** (see the superposition of the two optimized structures). Furthermore, the direct optimization of the peroxide position for the compound **2** starting from the side approach peroxide configuration of the compound **1** reveals that the peroxide molecule is squeezed from the side to the pop-up position that corresponds to the top initial complex.

Future detailed analysis of the role of the methoxy groups might need also to include electronic effects exerted by them. In addition to that, solvation effects and approaching trajectories of the substrate to the catalytic metal sites might be of importance for understanding of this reaction. Since the catalyst and the reactants and the products are all neutral we do not expect any significant changes of our qualitative results if a dielectric continuum model is used. It could be more informative to include explicit solvent molecules in the future studies not only in molecular dynamics calculations but also in dielectric model (supermolecule approach) to elucidate how a small peroxide molecule interacts with the catalytic metal sites. Hopefully, such extension of quantum

- (51) Linde, C.; Akermark, B.; Norrby, P.-O.; Svensson, M. *J. Am. Chem. Soc.* **1999**, *121*, 5083–5084.
(52) Strassner, T.; Houk, K. N. *Org. Lett.* **1999**, *1*, 419–421.
(53) Cavallo, L.; Jacobsen, H. *Angew. Chem., Int. Ed.* **2000**, *39*, 589–592.
(54) Brandt, P.; Norrby, P.-O.; Daly, A. M.; Gilheany, D. G. *Chem.—Eur. J.* **2002**, *8*, 4299–4307.
(55) No experimental data on activation energies of the discussed processes are available. One should keep in mind that the DFT approximation that is used in this work may lead to underestimation of TS barriers on a given spin surface.
(56) Abashkin, Y. G.; Burt, S. K.; Russo, N. *J. Phys. Chem. A* **1997**, *101*, 8085–8093.
(57) Schröder, D.; Shaik, S.; Schwarz, H. *Acc. Chem. Res.* **2000**, *33*, 139–145.
(58) Poli, R.; Harvey, J. N. *Chem. Soc. Rev.* **2003**, *32*, 1–8.

chemical studies would be useful to explain and predict effects of substitutions for the (salen)Mn catalyst on various positions.²⁸

Thus, on the basis of the detailed knowledge of the mode of action of the (salen)Mn^{III} catalase mimics, we suggest and rationalize structural changes of the catalyst that should lead to better therapeutic properties. Finally, we note that properties of the (salen)Mn^{III} compound, including the catalytic activity, can be tuned electronically with substitution of the axial ligand⁵⁹ and electron-donating/electron-withdrawing substituent changes on the salen framework.⁶⁰ Our findings on the reaction dismutation mechanism could be the starting point for further improvement of salen–manganese complexes as synthetic catalytic scavengers of reactive oxygen species.

Conclusions

A ping-pong mechanism approach has been considered to describe the H₂O₂ dismutation reaction with participation of (salen)Mn^{III} compound that acts as a nonpeptidyl mimic of catalase. Part I of the dismutation reaction—converting of a peroxide molecule into a water molecule with simultaneous oxidation of the metal atom of the catalyst—can be done quite effectively at the Mn catalytic center (the reaction TS barrier

= 3.6 kcal/mol). To act as catalytic scavengers of hydrogen peroxide, the oxomanganese salen complexes have to be deoxidized in the course of part II of the dismutation reaction. We show that there are two possible reaction routes for the second part of the dismutation reaction: the top and the side substrate approach routes. Our results suggest that the side approach reaction route for the catalyst recovery is the bottleneck for the whole dismutation process. We show that the catalyst could be at least temporarily deactivated (poisoned) if it entered the side approach reaction route due to formation of kinetically stable intermediate. On the basis of the detailed knowledge of the mode of action of the (salen)Mn^{III} catalase mimics, we suggest and rationalize structural changes of the catalyst that should lead to better therapeutic properties. The available experimental data support our conclusions.

Acknowledgment. The authors thank Dr. Brian T. Luke and Dr. Jack R. Collins for helpful discussions. This project has been funded in whole or in part with Federal funds from the National Cancer Institute, National Institute of Health, under Contract No. NO1-CO-12400. The content of this publication does not necessarily reflect the views or policies of the Department of Health and Human Services, nor does mention of trade names, commercial products, or organization imply endorsement by the U.S. Government.

IC048714O

(59) Adam, W.; Roschmann, K. J.; Saha-Möller, C. R.; Seebach, D. *J. Am. Chem. Soc.* **2002**, *124*, 5068–5073.

(60) Palucki, M.; Finney, N. S.; Pospisil, P. J.; Guler, M. L.; Ishida, T.; Jacobsen, E. N. *J. Am. Chem. Soc.* **1998**, *120*, 948–954.